Retraction

Retracted: An Operating Status Analysis System of Reactor Equipment Based on Voiceprint Recognition Technology

Journal of Control Science and Engineering

This article has been retracted by Hindawi following an investigation undertaken by the publisher [1]. This investigation has uncovered evidence of one or more of the following indicators of systematic manipulation of the publication process:

(1) Discrepancies in scope

(2) Discrepancies in the description of the research reported

(3) Discrepancies between the availability of data and the research described

(4) Inappropriate citations

(5) Incoherent, meaningless and/or irrelevant content included in the article

(6) Peer-review manipulation

The presence of these indicators undermines our confidence in the integrity of the article's content and we cannot, therefore, vouch for its reliability. Please note that this notice is intended solely to alert readers that the content of this article is unreliable. We have not investigated whether authors were aware of or involved in the systematic manipulation of the publication process.

Wiley and Hindawi regrets that the usual quality checks did not identify these issues before publication and have since put additional measures in place to safeguard research integrity.

We wish to credit our own Research Integrity and Research Publishing teams and anonymous and named external researchers and research integrity experts for contributing to this investigation.

The corresponding author, as the representative of all authors, has been given the opportunity to register their agreement or disagreement to this retraction. We have kept a record of any response received.

References

[1] L. Cao, H. Wei, Z. Huang, and M. Shi, "An Operating Status Analysis System of Reactor Equipment Based on Voiceprint Recognition Technology," *Journal of Control Science and Engineering*, vol. 2022, Article ID 7712649, 7 pages, 2022.

Hindawi

Research Article

An Operating Status Analysis System of Reactor Equipment Based on Voiceprint Recognition Technology

Litan Cao ⃝, Huabing Wei ⃝, Zhi Huang ⃝, and Minglei Shi ⃝

EHV Branch Company of State Grid Zhejiang Electric Power Co., Ltd, Zhejiang, Hangzhou 310007, China

Correspondence should be addressed to Litan Cao; 201704402@stu.ncwu.edu.cn

In order to find transformer (reactor) faults in time, a transformer working condition detection method and verification system based on voiceprint recognition technology was proposed. In this system, 73 groups of transformer audio were collected by the voice sensor on-site, with a total of about 1800 min. The recognition pattern based on a deep learning convolutional neural network was established. Through experiments, it was found that aiming at the additive superposition problem of transformer sound generated by a stable working condition and unstable instantaneous noise, a new method based on the cosine similarity algorithm was proposed to realize the separation detection of sound pattern superposition. The acoustic signals of the iron core under sinusoidal excitation were mainly frequency components of 100 Hz and 200 Hz. Harmonic excitation would aggravate the noise in this frequency band, and the third harmonic excitation had the greatest influence. Due to DC magnetic bias, the hysteresis loop of the iron core was distorted to a certain pole. In addition to the 100 Hz component, the odd harmonics of 150 Hz, 250 Hz, and 350 Hz and even harmonics of 200 Hz, 300 Hz, and 400 Hz also increased obviously. With the increase of direct current content, the performance of the noise signal became more prominent. A transformer working condition detection and verification analysis system was established.

1. Introduction

In recent years, with the rapid development of China's social economy, the demand for the power industry is also increasing year by year. With the continuous increase of the voltage level in the power system, the equipment demand of the high voltage system is also increasing and the requirements of the power system are becoming more stringent. During the 12th five-year plan period, the state grid held an annual meeting report, in which it clearly proposed that it planned to invest 2 trillion yuan in power grid construction, and the investment in UHV accounted for about 20% of the total amount [1]. Therefore, as one of the important power equipment in the power system, the demand for reactors in the market is becoming higher and higher. Voice recognition technology is the application of a speaker's voice and linguistic patterns based on physiological and behavioral characteristics. It differs from language recognition in such a way the technology does not recognize the spoken words itself. Instead, it identifies who is speaking by analyzing unique characteristics of the speech, such as the frequency of utterances. Voice recognition technology allows people to control access to restricted areas through their voice.

Power reactors can be divided into series reactors and parallel reactors according to the connection method. The former is mainly used to limit the short-circuit current, while the latter mainly plays the role of reactive compensation, such as absorbing capacitive reactive power in the network so as to provide reactive compensation for the system. In addition to the abovementioned functions, electric reactors also have the advantages of linear reactance, simple structure, light weight, low noise, convenient installation, and maintenance [2]. At present, dry-type hollow reactors account for about 75% of the 66 kV and below reactors, which are mainly used to limit short-circuit current and absorb capacitive reactive power in the power grid.

However, in the actual operation, with the continuous increase of the voltage level, the safety and stability

requirements of reactors are also higher and higher. Therefore, in the operation process of the power system, fire accidents caused by failure of reactors happen frequently. In the actual operation of the reactor, it is found by on-site statistics that the majority of the cases causing the above-mentioned accidents are winding short-circuits caused by the insulation defect of the reactor, which leads to fire [3]. Reactors are generally divided into a core type and a hollow type in the structure. For the core type reactors, the magnetic field will be generated in a certain space range occupied by the reactor during normal operation. And, the existence of the iron core will make most of the magnetic induction intensity be distributed in the core, so the magnetic leakage is very small. Fire accidents caused by failure of reactors occur frequently, which seriously affects the normal operation of substations. It is very necessary to find the fault and remove the faulty reactor from the system in the early stage of the reactor failure.

2. Literature Review

At present, the pulse oscillating voltage test is a very effective method to diagnose the interturn insulation of low-voltage reactors. This diagnosis method has been comprehensively and deeply elaborated in many pieces of literature of various countries, and its effectiveness has been proved by a large number of theories and field practices [4]. Ye et al. used a simulation model and mathematical derivation, respectively, to analyze the principle of the test in-depth and demonstrate its feasibility and effectiveness. The test could find signs of insulation failure of low-resistance winding well [5]. With the continuous development of power outage diagnosis methods, live detection technology was also rapidly developed and widely used in the fault diagnosis of UHV substations. Yermagambet et al. specifically described the development and application of ultrasonic partial discharge detection, high-frequency partial discharge detection, ultra-high frequency partial discharge detection, and other technologies in the fault diagnosis, search, and location of transformers and GIS equipment [6]. In recent years, in terms of a large number of literature on insulation aging and fire failure of low-voltage dry reactors, Zhang put forward specific rectification and preventive measures for operation and maintenance [7]. Xu et al. proposed measures such as strengthening the control of the raw materials, strengthening the control of the production process, strengthening the online detection and online monitoring means of dry reactors, actively carrying out the research and application of interturn short-circuit protection technology of dry reactor, and strengthening inspection and tests. By investigating new technologies such as phase-selective switching, power grid enterprises and equipment manufacturers strive to reduce the influence of circuit closing overvoltage and closing inrush current on low-voltage reactors, and improve the operating life of low-voltage reactors [8]. Ma et al. analyzed the reasons for the reactor to be easily burned by switching overvoltage and inrush current by combining the calculation of overvoltage and loop current generated when the branch

of the low-voltage reactor was put into operation. They proposed measures to limit the overvoltage and inrush current generated by the operation of parallel capacitor compensation devices [9]. Raj et al. proposed a technical scheme of phase-selective closing to suppress the adverse effects of inrush current and overvoltage on low-voltage reactor equipment, which had a good reference significance [10]. The feature detection in the voiceprint recognition system is to extract the basic features represented in the speech signal. This feature should be able to effectively distinguish different utterances and remain relatively stable to changes in the same utterance. Considering the quantification of features, the number of training samples and the evaluation of the system performance, current voiceprint recognition systems mainly rely on lower-level acoustic features for recognition.

Therefore, based on the voiceprint recognition technology, a transformer working condition detection and verification system was proposed. Through the collection of the voiceprint signal of a large power transformer (reactor), a voiceprint information corpus sample library was established. Through the analysis of the voiceprint signal, the voiceprint characteristics of the operation of the power transformer (reactor) devices were extracted. A transformer working condition detection and verification analysis system was established.

3. Research Methods

3.1. Acquisition, Preprocessing, and Characteristic Extraction of Transformer Voiceprint

3.1.1. Limitations. The extent of noise propagation is local. The noise energy emitted by the sound source propagates around, increasing with distance and being blocked by buildings. The intensity of the noise is quickly attenuated.

Noise pollution is transient. Different from the long-term residual accumulation of pollutant concentrations after the discharge of other pollution sources, once the noise source stops sounding, the noise is eliminated immediately, and there is no accumulation.

3.1.2. Data Collection. At present, there are relatively few equipment suitable for transformer (reactor) voiceprint collection. The power transformer (reactor) voiceprint collection equipment based on a microphone array sensor independently designed by a certain power grid technology was used to collect the voiceprint corpus. Its main advantages are that it can make full use of the space-time characteristics of the sound signal and has a strong anti-interference ability. It has good adaptability to transformer background noise, sound source location, and tracking. The main purpose of preprocessing is to measure the copper loss of the transformer, compare it with the data provided by the manufacturer, and achieve the purpose of checking the insulation and magnetic circuit between turns of the winding.

3.1.3. Transformer Voiceprint Data Preprocessing. First, the collected transformer audio was segmented [11]. In order to make the input transformer audio contain the same duration information, it was necessary to limit the duration. According to the need, segmentation of the transformer audio data was conducted. Since transformer voiceprint data were a series of discrete points and each point corresponded to a sampling point, the total length of the voiceprint data can be calculated using formula (1).

$$\text{Length}_{\text{data}} = time \times fs_{\text{sample}}. \tag{1}$$

In the abovementioned formula, fs_{sample} is the sampling frequency of the audio.

Second, the segmented transformer audio data were processed in a frame. A "frame" is the smallest unit of sound signal processing that was short enough in duration and contained enough sound characteristics. Sound signals were generally considered to be variable over long periods of time and invariant over short periods of time. For a very short time, the characteristics of sound could be regarded as fixed. Based on this idea, the whole transformer voiceprint data were further segmented [12]. In speech signal processing, the frame length was generally set to 50 ms, and the step length was generally 1/2 or 1/3 frame length. According to the experimental analysis, the transformer voiceprint changed less than the voice voiceprint. Therefore, the transformer voiceprint frame length was set to 500 ms and the step length was set to 1/2 frame length to reduce the amount of computation in data processing.

Finally, the transformer audio was windowed after frame splitting. Framing in reducing computational complexity at the same time also could bring a bad effect on the voice signal, which segmented the audio waveform directly (rectangular window), leading to the appearance of the sharp high-frequency signal in the border. Its general performance was the increase of the high-frequency harmonic component in the frequency spectrum, the appearance of the Gibbs effect, and an adverse effect on the subsequent signal processing. In order to reduce this effect, it is necessary to windoze the segmented data with endpoint smoothing, and use the Hamming window to windoze the frames. The function of the Hamming window is stated in formula (2).

$$\omega(n) = \begin{cases} 0.54 - 0.46\cos\left(\dfrac{2\pi n}{M-1}\right), & 0 \leq n \leq M-1, \\ 0, & \text{otherwise.} \end{cases} \tag{2}$$

3.1.4. Transformer Voiceprint Characteristic Extraction

(1) Energy Characteristics. Figure 1 shows the time-domain spectral line of the sound data of transformer operation, that is, the corresponding relationship between the time and waveform amplitude. In the analysis of sound signals. The amplitude of the instantaneous waveform corresponds to the
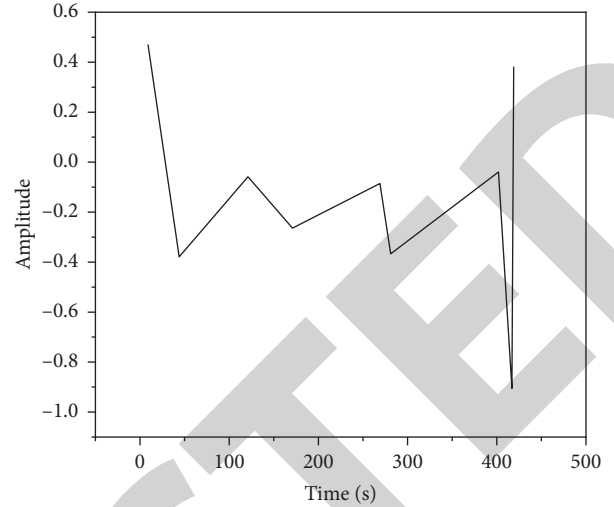

FIGURE 1: Time-domain spectral lines of sound data in transformer operation.

instantaneous energy of the data. Therefore, the greater the amplitude, the greater the energy. It can be seen from Figure 1 that these data have two peak values at the starting and ending points. And, the analysis shows that there is a large friction sound at these two points. Although this method can intuitively show the location of a large energy noise, it cannot distinguish sound abnormalities in other time domains. The energy characteristics cannot detect the location of the noise alone, which requires further analysis by other methods [13].

(2) Frequency Characteristics. In order to further analyze the vibration characteristics of the transformer sound waveform, it is generally considered that any sound can be decomposed into a series of trigonometric functions (sine function and cosine function) with different periods and amplitudes. The frequency and amplitude of a series of trigonometric functions are used to express the characteristics of this sound. This corresponding relationship has nothing to do with time, but it is related to frequency. Hence, the corresponding relationship with the time domain spectrum is called the frequency domain. The change from the time domain to the frequency domain is realized by Fourier Transform. The formula of Fourier transform is formula (3).

$$F(\omega) = \text{F}[f(t)] = \int_{-\infty}^{\infty} f(t)e^{-i\omega t}dt. \tag{3}$$

In formula (3), $f(t)$ is the time domain periodic function. $F(\omega)$ is the frequency domain function obtained after Fourier transform. The frequency domain waveform shown in Figure 2 is obtained from the time domain waveform shown in Figure 1 obtained by Fourier transform.

(3) Mayer Coefficient. Mayer frequency is an auditory characteristic that simulates the human ears. It grows rapidly in the low-frequency range, but slowly in the high-frequency
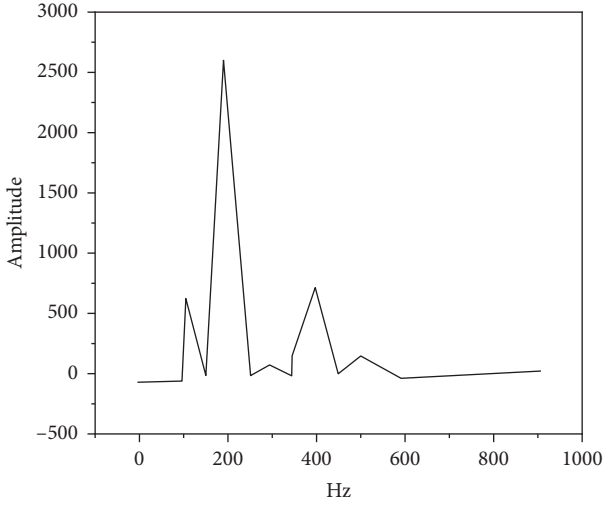
Figure 2: Spectrum lines in the frequency domain of sound.

range [14]. The corresponding relationship between the frequency and Mayer frequency is shown in formula (4).

$$\text{mel}(f) = 2595\log_{10}\left(\frac{f}{700} + 1\right). \qquad (4)$$

Meir frequency conversion and characteristic extraction are generally implemented by Meir filter banks, which generally contain a series of triangular filters set according to Meir frequency conversion relations. Each filter has the same bandwidth $f\text{melband} = (\text{mel}(fh) - \text{mel}(fl))/(N + 2)$ in Meir frequency, where fh and fl are the highest frequency and lowest frequency in the frequency range, respectively.

In 4000 Hz, 24 Mayer filters were used for the experiment. The Mayer frequency coefficient of the 500 ms frame length is shown in Figure 3. After DCT, MFCC is obtained, as shown in formula (5).

$$c(n) = \sum_{m=0}^{N-1} s(m) \cos\left(\frac{\pi n(m - 0.5)}{M}\right), n = 1, 2, \ldots, L. \qquad (5)$$

(4) Frequency Compression. Although the MEL frequency coefficient has an advantage of dimension reduction and a good high-frequency compression effect, there still exists the problem of shortage of the low-frequency resolution. Namely, in the low frequency, even if the resolution has been corresponding to the transformer working frequency, it cannot distinguish the abnormal working frequency signal. Although it can judge the working characteristics of the current transformer correctly, it cannot accurately judge whether there is an abnormal working frequency noise. Therefore, it is necessary to further increase the low-frequency resolution. Based on the idea of "changing resolution from high to low" of Mayer frequency, a similar frequency compression strategy is adopted, which can be divided into the following three steps:

Step1: divide sound information into three frequency bands: low frequency, middle frequency, and high frequency.

Step2: use different frequency compression ratios for the three frequency bands.

Step3: adopt the maximum compression strategy and select the maximum value of each compression interval as the compression result [15].

3.2. Transformer Voiceprint Similarity Detection Algorithm. It is assumed that the sound collected in transformer working condition is additively superimposed by the sound from stable working condition and unstable instantaneous noise, and the possible mutual interference is ignored. At the same time, the following assumptions are made in the transformer voiceprint experiment.

Hypothesis 1. A piece of audio should be similar most of the time, i.e., unstable signals are very few in comparison and very different from stable signals.

Hypothesis 2. Continuous noise can be considered a stable signal when its frequency is greater than the frame sampling frequency (2 Hz, i.e., 500 ms/frame) [16].

Hypothesis 3. Unstable signals should be instantaneous signals, or signals that last for a short time, or signals with large intervals.

In Hypothesis 1, the cosine similarity algorithm is used to calculate the similarity of each characteristic vector in the audio. Cosine similarity is an algorithm to evaluate the similarity by calculating the cosine value of the included angle of two vectors. According to the Euclidean vector dot product formula, as shown in formula (6).

$$A \cdot B = \|A\|\|B\| \cos \theta. \qquad (6)$$

In formula (6), θ is the angle between vector A and vector B in space. The similarity between vector $A = [A_1, A_2, \ldots, A_N]$ and vector $B = [B_1, B_2, \ldots, B_N]$ can be obtained, as shown in formula (7).

$$\text{Similarity} = \cos\theta = \frac{A \cdot B}{\|A\|\|B\|} = \frac{\sum_{i=1}^{N} A_i \times B_i}{\sqrt{\sum_{i=1}^{N} (A_i) \times \sum_{i=1}^{N} (B_i)}}. \qquad (7)$$

In order to separate an audio segment into a stable part and an unstable part, a similarity displacement algorithm is proposed.

3.3. Convolutional Neural Network Pattern Recognition Based on Deep Learning

3.3.1. Mel Time Spectrum-CNN Identification Model. The noise signal of the iron core can represent the operating state information of the iron core reflected by the vibration signal. Under different operating conditions, the noise signal of the iron core will change greatly in the time domain and frequency domain. But the operating state information is very complicated and difficult to distinguish directly.

The core acoustic signal is preprocessed and the Mel time-spectrum is used as the input of the CNN network for
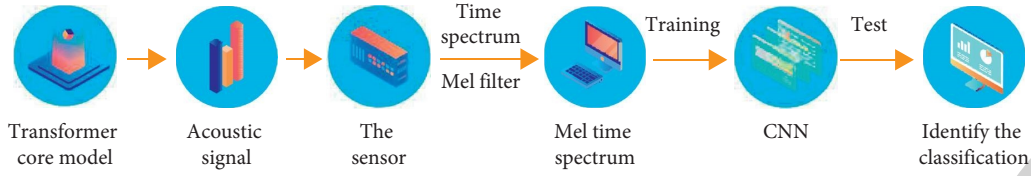
Figure 3: Structure diagram of the Mel time spectrum-CNN vowel recognition model.

Table 1: Distribution of core sound database sample.

Operating conditions	The label	Number of training sets	Number of testing sets
Sine excitation	1	400	100
Harmonic excitation	2	320	80
DC bias	3	400	100
Total		1120	280

deep learning, forming the Mel time-spectrum-CNN recognition model and realizing the extraction of voice print characteristics and pattern recognition of different operating states. Figure 3 shows the structure of the Mel time spectrum-CNN vowel recognition model. The Mel time spectrum is used as the input quantity representing the sound signal of the iron core. The input image pixel is $188 \times 40 \times 3$ dimensions (width × height × depth), where the input width 188 represents the time component of the sound signal of the iron core, the input height 40 represents the frequency domain component of the sound signal of the iron core at the Mel Frequency Scale and input depth 3 represents the RGB color channel represented by the energy spectral density of the iron core acoustic signal. After the images are successively input into the CNN network, the convolutional neural network performs cross learning and characteristic extraction on the Mel time spectrum samples under various operating states. And, it finally generalizes the weight model capable of pattern recognition to realize the recognition and classification of iron cores under different operating states [17].

3.3.2. The Data Set. In order to verify the effectiveness of the Mel time spectrum-CNN identification model, all the sound data collected in the experimental scheme were preprocessed in batches. The results were made into the training set and the test set of the model. The sample distribution of the data set is shown in Table 1.

Under the excitation of different voltage levels, harmonic number, or DC content, the characteristics of the transformer voiceprint pattern showed a certain trend of change. In the research, the data under the same working conditions were classified into one class and unified labels were carried out. And, the characteristic quantity without parameters was learned through the convolutional neural network. In order to verify the generalization characteristic ability of the model, 20% of the samples of each type were randomly selected as a testing set to verify the validity of the model, and the remaining 80% as a training set to train the model [18]. In addition, in order to avoid network overfitting, samples of all types and corresponding labels were randomly sorted as

data sets, which were input into the deep learning network in a disordered order to ensure the effectiveness of learning [19].

3.3.3. Network Structure. In the research, according to the size and characteristics of the data set, a network structure was designed to deal with the characteristic extraction of the transformer core sound pattern. The network structure could achieve ideal recognition accuracy with better performance, and avoid problems such as over-fitting and gradient explosion while taking into account the stability of training. The network structure used in the research is shown in Table 2.

In the customized CNN network, in order to prevent overfitting, a dropout operation was carried out in the two-layer fully connected layer. The dropout operation randomly dropped some neurons through probability, so that the acoustic pattern text could carry out parameter iteration while keeping the number of input and output neurons unchanged [20]. In addition, the activation function ReLU greatly improved the training speed of the network, and the batch normalized operation solved the problem of neuronal compatibility, which greatly improved the performance and stability of the network.

4. Result Analysis

Based on transformer voiceprint acquisition, processing, characteristic extraction, and separation detection algorithm, a transformer working condition detection and verification system with a user interface was constructed. The user could select the input audio and set the threshold value of each analysis part according to the situation. Finally, the analysis result of the audio was output.

The characteristic of the Adadelta optimizer is that it can adjust the learning rate adaptively. In the early stage of training iteration, the learning rate is enlarged when the gradient is small. And in the middle and late stages, the learning rate is slowed down when the gradient is large, so as to realize the adaptive adjustment, and then realize the optimal iteration. The comparison of hyperparameter

TABLE 2: CNN network structure used for transformer core voiceprint recognition.

| Layer type	Number of channels	Core/moving step length	Activation function/pooled type/batch normalization/dropout
Input	3		Batch normalization
Convolution layer	32	3 × 3/1	ReLU, batch normalization
Pooling layer	32	3 × 3/2	Max pooling
Convolution layer	64	3 × 3/1	ReLU
Pooling layer	64	2 × 2/2	Max pooling
Convolution layer	128	3 × 3/1	ReLU
Pooling layer	128	2 × 2/2	Max pooling, batch normalization
The connection layer	1024		Dropout
The connection layer	1024		Dropout, softmax
Output	3		
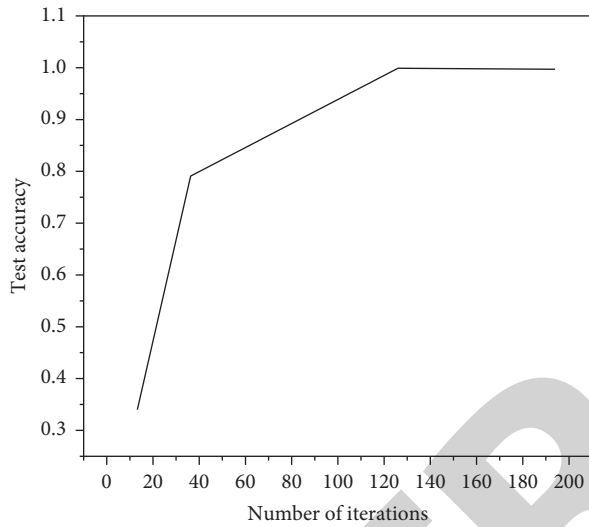
FIGURE 4: Comparison of recognition accuracy between Adadelta and different loss function combinations.

combination identification effects of Adadelta and a variety of loss functions is shown in Figure 4. As shown in Figure 4, except for the normalized absolute mean error (mape) function (the calculation was withdrawn at the 90th iteration because the loss value did not decrease for 50 consecutive iterations), all the other combinations achieved high recognition accuracy. But in terms of learning speed, categorical cross entropy was the best.

The acoustic signals of the core under sinusoidal excitation were mainly frequency components of 100 Hz and 200 Hz. Harmonic excitation would aggravate the noise in this frequency band and the third harmonic had the greatest influence. Due to the DC magnetic bias, the hysteresis loop of the iron core was distorted to a certain pole. In addition to the 100 Hz component, the odd harmonics of 150 Hz, 250 Hz, and 350 Hz, and even harmonics of 200 Hz, 300 Hz, and 400 Hz also increased obviously. With the increase of the DC content, the performance of the noise signal became more prominent. The calculation of Pearson's correlation coefficient showed that the vibration signal of the iron core had a high similarity with the sound signal, and the correlation coefficient was up to 0.701. The sound signal could represent the operating state information of the core reflected by the vibration signal.

5. Conclusions

The acoustic signal of the iron core under sinusoidal excitation is dominated by frequency components of 100 Hz and 200 Hz. Harmonic excitation will aggravate the noise in this frequency band, of which the third harmonic has the greatest impact; due to the DC bias, the iron core hysteresis loop distorts to a certain pole, in addition to the 100 Hz component, the odd harmonics such as 150 Hz, 250 Hz, and 350 Hz and the even harmonic components such as 200 Hz, 300 Hz, and 400 Hz also increase significantly, and with the DC content increases, the performance of the noise signal becomes more prominent. It is reflected in the completion of online monitoring. While monitoring can realize noncontact detection, the voiceprint sensor layout is more flexible, signal acquisition does not produce electromagnetic signals, and will not interfere with the normal operation of the equipment. The future work will focus on improving the accuracy and timeliness of the transformer operation fault identification algorithm and further improving the function of the transformer working condition detection and verification system. At present, although the function of long-term working condition tracking and judgment of transformer can be added theoretically, the existing system cannot verify the feasibility of its stable operation due to the lack of long-term observation data of the same transformer. In the next step, in addition to strengthening the collection and acquisition of corpus data samples of different potential fault types during the operation of the same type of transformer, it is also necessary to strengthen the construction of a corpus of operation voiceprint data of different types of transformers, so as to provide a sample accumulation of big data for the application of voiceprint recognition technology in transformer working condition detection.

Data Availability

The data used to support the findings of this study are available from the corresponding author upon request.

Conflicts of Interest

The authors declare that they have no conflicts of interest.

Acknowledgments

References

[1] S. Yang, Y. Feng, N. Liu et al., "Enhancement on the removal of rhodamine b (rhb) by means of the enlarged anode electric biological (eaeb) reactor," *Chemosphere*, vol. 245, Article ID 125566, 2020.

[2] F. J. C. M. Beckers, T. Huiskamp, A. J. M. Pemen, and E. J. M. van Heesch, "Energizing a long nanosecond pulsed corona reactor: electrical characterization," *IEEE Transactions on Plasma Science*, vol. 48, pp. 500–511, 2020.

[3] A. Sharma and R. Kumar, "A Framework for Pre-computed Multi- Constrained Quickest QoS Path Algorithm," *Journal of Telecommunication, Electronic and Computer Engineering*, vol. 9, 2017.

[4] F. Yuan, K. Lv, B. Tang et al., "Optimization design of oil-immersed iron core reactor based on the particle swarm algorithm and thermal network model," *Mathematical Problems in Engineering*, vol. 2021, no. 4, pp. 1–14, 2021.

[5] M. O. Ye and K. Somnuk, "Continuous hydrosonic reactor for methyl esters production process from low free fatty acid oil using 3d-printed rotor," *Materials Science Forum*, vol. 998, pp. 140–145, 2020.

[6] B. T. Yermagambet, M. K. Kazankapova, B. K. Kasenov, A. Z. Aitmagambetova, and E. E. Kuanyshbekov, "Synthesis of graphene-containing nanomaterials based on a carbon product using electric arc discharge," *Solid Fuel Chemistry*, vol. 55, no. 6, pp. 380–390, 2021.

[7] W. Zhang, D. Zhang, X. Liu, W. Tian, S. Qiu, and G. H. Su, "Thermal-hydraulic analysis of the thermoelectric space reactor power system with a potassium heat pipe radiator," *Annals of Nuclear Energy*, vol. 136, Article ID 107018, 2020.

[8] Z. J. Xu, R. F. Wang, J. Wang, and D. H. Yu, "Parkinson's disease detection based on spectrogram-deep convolutional generative adversarial network sample augmentation," *IEEE Access*, vol. 8, pp. 206888–206900, 2020.

[9] H. Ma, Y. Zuo, T. Li, and C. L. P. Chen, "Data-driven decision-support system for speaker identification using e-vector system," *Scientific Programming*, vol. 2020, no. 1, pp. 1–13, 2020.

[10] M. S. Pradeep Raj, P. Manimegalai, P. Ajay, and J. Amose, "Lipid data acquisition for devices treatment of coronary diseases health stuff on the internet of medical things," *Journal of Physics: Conference Series*, vol. 1937, no. 1, Article ID 012038, 2021.

[11] S. Marwaha and K. Ghosh, "Analytical modeling of diffusion of moisture in silicon photovoltaic module under damp heat testing condition," *Silicon*, vol. 14, no. 9, pp. 4757–4766, 2021.

[12] Q. Wang, K. Zheng, H. Yu, L. Zhao, X. Zhu, and J. Zhang, "Laboratory experiment on the nano-tio 2 photocatalytic degradation effect of road surface oil pollution," *Nanotechnology Reviews*, vol. 9, no. 1, pp. 922–933, 2020.

[13] X. Liu, C. Ma, and C. Yang, "Power station flue gas desulfurization system based on automatic online monitoring platform," *Journal of Digital Information Management*, vol. 13, no. 06, pp. 480–488, 2015.

[14] A. N. Nazarychev, E. M. Novoselov, D. A. Polkoshnikov, A. S. Strakhov, and A. A. Skorobogatov, "A method for monitoring the condition of rotor windings in induction motors during startup based on stator current," *Russian Journal of Nondestructive Testing*, vol. 56, no. 8, pp. 661–667, 2020.

[15] P. Bhukya and D. Basak, "Nondestructive evaluation of track and haulage ropes of aerial ropeway installation in India-a case study," *Russian Journal of Nondestructive Testing*, vol. 56, no. 11, pp. 927–935, 2020.

[16] R. Huang, P. Yan, and X. Yang, "Knowledge map visualization of technology hotspots and development trends in China's textile manufacturing industry," *IET Collaborative Intelligent Manufacturing*, vol. 3, no. 3, pp. 243–251, 2021.

[17] P. Zapico, G. Valiño, J. C. Rico, V. M. Meana, and P. Fernández, "On-machine non-contact roughness verification system based on conoscopic holography," *Precision Engineering*, vol. 73, pp. 115–127, 2022.

[18] Y. Y. Park, N. H. Lee, N. D. Kim, W. J. Kim, and J. Shin, "The development of verification system for interoperability in digital substation," *The Transactions of the Korean Institute of Electrical Engineers*, vol. 69, no. 11, pp. 1633–1639, 2020.

[19] D. Borio, "An experimental evaluation of global navigation satellite system/inertial navigation system-verification strategies for vehicular applications," *IEEE Intelligent Transportation Systems Magazine*, vol. 12, no. 3, pp. 25–35, 2020.

[20] Z. Guo and Z. Xiao, "Research on online calibration of lidar and camera for intelligent connected vehicles based on depth-edge matching," *Nonlinear Engineering*, vol. 10, no. 1, pp. 469–476, 2021.